Surface formation routes of interstellar molecules : a laboratory study

Sergio, I.

CHAPTER 7

Competition between CO and O_2-ice hydrogenation channels and surface formation of CO_2 at low temperatures[1]

In the past decade astrochemical laboratory studies have focused on the investigation of isolated surface reaction schemes, starting from the hydrogenation of simple and pure ices, like solid CO or O_2. The reaction products observed for CO hydrogenation are H_2CO and CH_3OH, while after O_2 hydrogenation H_2O_2 and H_2O are formed. We present here the first systematic laboratory study focusing on H-atom addition to a mixed CO:O_2 ice. Mixed ices are more relevant from an astrochemical point of view and can elucidate reactions with radicals that are not readily studied otherwise. The aim of this chapter is to investigate the competition between CO and O_2 hydrogenation, and the corresponding surface formation of CO_2 for astronomically relevant temperatures. Mixtures of CO:O_2 = 4:1, 1:1 and 1:4 are deposited on a substrate in an ultra high vacuum setup at low temperatures (15 and 20 K) and subsequently hydrogenated. The ice is monitored by means of Reflection Absorption InfraRed Spectroscopy (RAIRS). The results show that the contemporary presence of CO and O_2 molecules in the ice influences the final product yields of the separate CO + H and O_2 + H channels, even though the formation rates are not significantly affected. CO_2 is efficiently formed through dissociation of the HO-CO intermediate complex in all studied CO:O_2 mixtures and within the experimental uncertainties no dependency on temperature or ice composition is observed. Moreover, the CO + O and HCO + O channels are not efficient at low temperature under our experimental conditions. The laboratory results demonstrate that CO_2 can be formed in interstellar ices at low temperatures in the absence of UV radiation and show a correlation between the formation of CO_2 and H_2O, which is consistent with the astronomical observation of solid CO_2 in water-rich environments.

[1]Based on: S. Ioppolo, Y. van Boheemen, H. M. Cuppen, E. F. van Dishoeck, and H. Linnartz, 2010, submitted to Monthly Notices of the Royal Astronomical Society

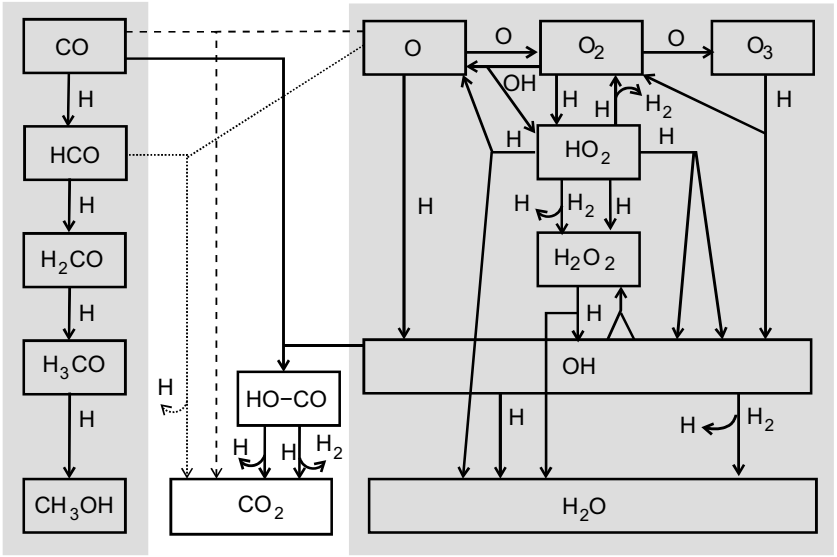

Figure 7.1 A schematic representation of the reaction network as discussed in the present study. The CO + H channel (Chapter 2) is shown on the left-side of the figure, while the $O/O_2/O_3$ + H channels are plotted as presented in Chapter 5 on the right-side. The possible CO_2 formation routes are shown in between the CO + H and $O/O_2/O_3$ + H channels: the dissociation of the HO-CO intermediate (*solid arrow*) is one of the topics of this work; the hydrogenation of the HO-CO complex (*solid arrow*) is presented in Chapter 8; the suggested CO + O (*dashed arrow*) and HCO + O (*dotted arrow*) routes are not experimentally confirmed at low temperature (Tielens & Hagen 1982, Ruffle & Herbst 2001).

7.1 Introduction

Infrared Space Observatory and *Spitzer Space Telescope* observations have shown that H_2O, CO, CO_2, and, in some cases, CH_3OH represent the bulk of solid-state species in dense molecular clouds and star-forming regions. Other ice components, such as CH_4, NH_3, OCN^-, H_2CO, HCOOH, SO_2, and OCS have abundances <5% relative to H_2O (*e.g.*, Gibb et al. 2004, Boogert et al. 2008, Pontoppidan et al. 2008, Öberg et al. 2008, Zasowski et al. 2009, Bottinelli et al. 2010). Several of these species are assumed to be formed in solid state reactions on the surfaces of icy dust grains, first outlined by Tielens & Hagen (1982). Although these reactions have been postulated nearly 30 years ago, few have been measured in the laboratory at low temperatures and UHV conditions until recently. Over the past decade, detailed laboratory studies have started to investigate isolated surface reaction schemes, starting from the hydrogenation of simple and pure ices, like solid CO or O_2.

Several groups proved that the hydrogenation of CO ice at low temperatures (12–20 K)

leads to the subsequent formation of H_2CO and CH_3OH (*e.g.*, Watanabe et al. 2004, 2006a, Fuchs et al. 2009). The experiments showed that this hydrogenation process involves only the upper monolayers (4 ML, where 1 ML corresponds to 10^{15} molecules cm^{-2}) of the CO ice and formation rates drop at temperatures higher than 15 K, since the desorption of H atoms becomes important at these temperatures. The hydrogenation of CO to CH_3OH proceeds in four steps,

$$CO \xrightarrow{H} HCO \xrightarrow{H} H_2CO \xrightarrow{H} H_3CO \xrightarrow{H} CH_3OH, \tag{7.1}$$

where the first step from CO to HCO and the third step from H_2CO to H_3CO have a barrier.

The other surface reaction channel that has been well investigated is the hydrogenation of O_2 ice, which leads to the formation of H_2O_2 and H_2O (*e.g.*, Miyauchi et al. 2008, Ioppolo et al. 2008, 2010, Cuppen et al. 2010). This hydrogenation process

$$O_2 \xrightarrow{2H} H_2O_2 \xrightarrow{2H} 2H_2O \tag{7.2}$$

behaves differently compared to the hydrogenation of CO ice (reaction scheme 7.2 shows the simplified version of this route, as discussed by Tielens & Hagen 1982). In this case, the penetration depth of H atoms in the O_2 ice increases with temperature, even at values close to the desorption temperature of the O_2 layer, involving the bulk of the ice (tens of monolayers). Thus, H atoms trapped in the ice can diffuse and eventually react up to much higher temperatures. Moreover, at least the formation of H_2O_2 does not exhibit any noticeable barrier.

The present work is a further step towards a laboratory investigation of surface reactions in a more complex and realistic interstellar ice analogue by studying the competition between the two hydrogenation channels in a binary CO:O_2 ice mixture as well as the inherent formation of solid CO_2. The latter is not found as a reaction product for the separate channels. CO_2 is one of the most common and abundant ices, yet its formation routes are still very uncertain. Figure 7.1 shows a schematic representation of all the reaction networks investigated in this work (*solid arrows*) and links the previously studied CO + H and O_2 + H channels through the observed CO_2 formation. The dashed and dotted arrows represent suggested CO_2 formation routes in the networks of Tielens & Hagen (1982) and Ruffle & Herbst (2001), that are not experimentally confirmed at low temperature in our studies. As discussed in § 7.4.4, CO_2 is formed under our experimental conditions through the reaction CO + OH. Here OH radicals are formed through the hydrogenation of O_2 ice, while in space they can also result from the O + H reaction or from photodissociation of H_2O ice. Our experiments are designed to test the interaction of the aforementioned individual surface reaction channels rather than simulate a complete realistic interstellar ice evolution. Hence, our experiments show that OH radicals can get further hydrogenated, leading to H_2O formation, or, alternatively, can react with the CO present in the ice, forming solid CO_2. These results give the experimental evidence for the correlation of H_2O and CO_2 formation. Indeed, observations by the *Infrared Space Observatory* (*e.g.*, Gerakines et al. 1999, Nummelin et al. 2001, Gibb et al. 2004) and the

Spitzer Space Telescope (*e.g.*, Boogert et al. 2004, Bergin et al. 2005, Pontoppidan et al. 2005, 2008, Whittet et al. 2007) show that roughly $\frac{2}{3}$ of the solid CO_2 observed in quiescent molecular clouds and star-forming regions is found in water-rich environments, suggesting that the formation routes of these two molecules are linked. The remaining CO_2 ice is predominantly found in a H_2O-poor, CO-rich environment (Pontoppidan et al. 2008). The origin of this common ice mantle component remains uncertain.

It is widely accepted that CO_2 is not formed efficiently in the gas phase, with subsequent accretion onto the grains ($CO_2^{gas}/CO_2^{ice} \ll 1$; van Dishoeck et al. 1996, Boonman et al. 2003). Therefore, the observed CO_2 most likely has to be formed in the solid phase. Several reaction mechanisms have been proposed with a relevance depending on astronomical environment. Energetic processing, such as UV and ion irradiation of interstellar ice analogues, has been investigated in various laboratories and proposed as an efficient CO_2 formation mechanism (Chapter 9 and references therein). Furthermore, in the absence of UV irradiation several cold solid-phase reaction channels have been reported in the past decades as an alternative formation mechanism to explain the CO_2 abundance observed in cold clouds (*e.g.*, Tielens & Hagen 1982, Ruffle & Herbst 2001, Stantcheva & Herbst 2004, Fraser & van Dishoeck 2004, Goumans et al. 2008, Goumans & Andersson 2010). The most straightforward surface reaction channel is the addition of an O atom to solid CO ice. The reaction CO + O $\rightarrow$ CO_2 has been experimentally investigated only by temperature programmed desorption experiments using thermal O atoms below 160 K (Roser et al. 2001) and by energetic O atoms (Madzunkov et al. 2006). This surface reaction channel has a high reaction barrier, because the $CO(^1\Sigma)$ + $O(^3P)$ reactants do not correlate directly with the singlet ground state $CO_2(^1\Sigma)$ (2970 K in the gas phase; Talbi et al. 2006). Ruffle & Herbst (2001) found in their astrochemical model that they were only able to reproduce the CO_2 abundances observed towards the cold (10 K) cloud Elias 16, if they artificially lowered the barrier to 130 K. Recently, Goumans & Andersson (2010) used harmonic quantum transition state theory to conclude that whilst quantum mechanical tunneling through the activation barrier increases the classical reaction rate for reaction CO + O at low temperatures (10−20 K), the onset of tunneling is at too low temperatures for the reaction to efficiently contribute to CO_2 formation in quiescent clouds.

Solid CO_2 is further suggested to be formed through the surface reaction HCO + O, which presents two exit channels (CO_2 + H and CO + OH; Ruffle & Herbst 2001). Alternatively, solid CO_2 can be formed through the surface reaction CO + OH, which yields a HO-CO intermediate. This complex can directly dissociate, forming solid CO_2 and leaving a H atom, or can be stabilized by intramolecular energy transfer to the ice surface and eventually react with an incoming H atom in a barrierless manner to form CO_2 and H_2 (Goumans et al. 2008). Oba et al. (2010) investigated the reaction CO + OH depositing CO molecules on a cold substrate (10 and 20 K) together with H_2O fragments (OH, H, O and H_2) produced by dissociating H_2O molecules in a microwave source. They confirmed the formation of solid CO_2 at low temperature by using CO and OH beams to initiate surface reactions on a cold substrate. However, their experiments differ from ours. In the present work we hydrogenate CO:O_2 ices and OH radicals are produced in the ice through the O_2 + H channel. Therefore, our experiments give also hints on the interaction

between different surface reaction channels. In chapter 8 we investigated experimentally the hydrogenation of the HO-CO complex, which presents three exit channels (CO_2 + H_2, HCOOH, H_2O + CO) with a branching ratio purely statistical as suggested by density functional theory models and in agreement with our experimental results (Goumans et al. 2008, Ioppolo et al. 2010a). In the present study the HO-CO complex itself is not observed in the ices under our experimental conditions, since it is efficiently dissociated to form CO_2. More details are reported in § 7.4. First, in § 7.2 and 7.3 the experimental method and data analysis are discussed.

7.2 Experimental details

The experiments are performed using an ultra high vacuum setup (SURFRESIDE), which consists of a main chamber (10^{-10} mbar) and an atomic beam line. Details are available in Chapters 2 and 4. The ice is grown on a gold coated copper substrate (12−300 K) that is mounted on the cold head of a close-cycle He cryostat. Deposition of selected $^{12}C^{16}O$:$^{16}O_2$ mixtures (4:1, 1:1 and 1:4) proceeds under an angle of 45° and with a rate of 0.7 ML min^{-1}. The interstellar solid CO:O_2 mixing ratio is observationally constrained to >1:1 (Pontoppidan et al. 2003). After deposition the ice mixture is exposed to a cold H-atom beam. H_2 molecules are dissociated into the capillary of a well-characterized thermal cracking source (Tschersich & von Bonin 1998, Tschersich 2000, Tschersich et al. 2008), which is used to hydrogenate the sample. A quartz pipe with a nose-shaped form is placed along the path of the dissociated beam to efficiently thermalize all H atoms to room temperature through surface collisions before they reach the ice sample. In this way, hot species (H; H_2) cannot reach the ice directly. Furthermore, the relatively high temperature of 300 K of the incident H atoms in our experiments does not affect the experimental results, since H atoms are thermally adjusted to the surface temperature as has been shown in Chapter 2. The final H-atom flux (2.5×10^{13} atoms cm^{-2} s^{-1}) is measured at the substrate position in the main chamber using a quadrupole mass spectrometer, following the procedure as described in the Appendix A of Chapter 4. The absolute error in the H-atom flux determination is within 50%. Ices are monitored by means of Reflection Absorption InfraRed Spectroscopy (RAIRS) using a Fourier Transform InfraRed spectrometer (FTIR), which covers the range between 4000 and 700 cm^{-1} (2.5−14 μm). A spectral resolution of 1 cm^{-1} is used and 128 scans are co-added. RAIR difference spectra (ΔA) relative to the initial unprocessed CO:O_2 ice are acquired every few minutes during H-atom exposure.

We performed a control experiment at 15 K in which a CO:O_2 ice is exposed to an H_2 molecular beam (*i.e.*, without H atoms) to show that the products detected in the hydrogenation experiments are formed on the surface and do not originate from background deposition. Only H_2O is detected in this experiment, which gives us an estimate for the background contamination, that is negligible. None of the other products are detected in this way. It should be noted that we use in the present experiments the same H-atom flux as used in Chapters 2 and 4. Therefore, the hydrogenation of our mixtures involves effectively a lower H-atom flux per (CO and O_2) channel.

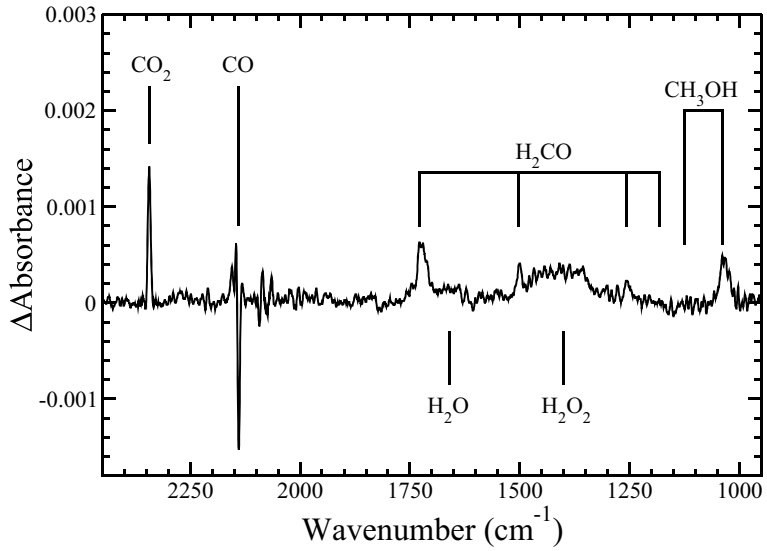

Figure 7.2 RAIR difference spectrum of the CO:O_2=1:4 ice, with respect to the spectrum before H-atom addition, at 15 K after a H-atom fluence of 1.3×10^{17} atoms cm^{-2}.

7.3 Data analysis

Figure 7.2 shows a RAIR difference spectrum of a CO:O_2 = 1:4 mixture acquired after a H-atom fluence (flux × time) of 1.3×10^{17} atoms cm^{-2}. The negative peak shown in Fig. 7.2 is caused by the CO use-up in surface reaction processes. O_2 is infrared in-active, and therefore cannot be observed in the infrared spectrum. All the final reaction products obtained from the hydrogenation of a pure CO ice (H_2CO and CH_3OH; *e.g.*, Watanabe et al. 2004, 2006a, Chapter 2) and a pure O_2 ice (H_2O and H_2O_2; *e.g.*, Miyauchi et al. 2008, Chapters 3 and 4) are present. Neither the intermediate species from the separate CO and O_2 channels, like HCO, H_3CO, HO_2, OH, and O_3, nor more complex species, like the stabilized HO-CO intermediate, HCOOH, and H_2CO_3[1], are observed. However, a new feature appears at ~2344 cm^{-1}, which belongs to the asymmetrical stretching mode of CO_2 ice. This molecule is formed in all our performed experiments at 15 and 20 K, with different CO:O_2 mixing ratios, but was not found in the previous CO + H or O_2 + H experiments.

The infrared spectra are reduced to obtain the column densities of the newly formed species. As a first step in the infrared data analysis, a straight baseline is subtracted from all spectra. Some absorption features, like the H_2O bending mode (~1650 cm^{-1}) and the H_2CO ν(C=O) stretching mode (~1720 cm^{-1}) suffer from spectral overlap. Here a multi-Gaussian fit is used to determine the area of the selected bands. Since the asymmetric 1440 cm^{-1} H_2O_2 band overlaps with the 1500 cm^{-1} H_2CO band, a spectrum of pure H_2O_2

[1]Solid H_2CO_3 is observed only in control experiments presented in Chapter 8.

ice is fitted in addition to a Gaussian to our infrared spectrum. The spectrum of solid H_2O_2 is obtained as discussed in Chapter 5, by co-depositing H atoms and O_2 molecules with a ratio of $H/O_2 = 20$ and subsequently heating the ice to a temperature higher than 30 K, which is just above the O_2 desorption temperature (Acharyya et al. 2007).

The column density N_X (molecules cm^{-2}) of species X in the ice is calculated using: $N_X = \int A(\nu)d\nu / S_X$, where $A(\nu)$ is the wavelength dependent absorbance. Since literature values of transmission band strengths cannot be used in reflection measurements, an apparent absorption band strength, S_X of species X is determined by individual calibration experiments. These have been described in detail in Chapters 2, 4 and 5. Like for CO, CH_3OH and H_2O, an isothermal desorption experiment has been performed to determine the apparent absorption band strength of CO_2 by determining the transition from zeroth-order to first-order desorption. This is assumed to occur at the onset to the submonolayer regime and appears in the desorption curve as a sudden change in slope. Since pure H_2CO and H_2O_2 are experimentally difficult to deposit, because of their chemical instability, the values for S_{H_2CO} and $S_{H_2O_2}$ are obtained by assuming mass balance as reported in Chapters 2 and 5, respectively.

7.4 Results and discussion

7.4.1 Hydrogenation of O_2 molecules

Figure 7.3 shows the H_2O_2 (*top panels*) and H_2O (*bottom panels*) column densities as a function of the H-atom fluence for the three different mixing ratios ($CO:O_2$ = 4:1 *circles*, 1:1 *squares* and 1:4 *triangles*) and two temperatures investigated (15 K *left panels* and 20 K *right panels*). For comparison, results from the hydrogenation of pure O_2 ice (Chapter 4) are also plotted (*diamonds*). Note that the top-right panel has a different scale for the column density than the other three diagrams. Formation rate and final yield of H_2O_2 and H_2O for all the investigated mixtures are lower than those from the pure O_2 ice hydrogenation. The differences in the final yield are more evident at higher temperature, where the yield for the mixed ices only moderately increases, whereas it increases with several monolayers for the pure O_2 experiments. This cannot be explained only by a low effective H-atom flux for the O_2 channel. Hence, the presence of CO in the mixture influences the final results. In Chapter 2 we showed that H atoms can penetrate only a few layers of CO ice. Therefore, the presence of CO in the mixture most likely diminishes the penetration depth of H atoms into the ice compared to O_2 + H, and, therefore, desorption of H atoms from the ice can become important at higher temperatures. This explains the difference in the H_2O_2 and H_2O final yields compared to those from the pure O_2 ice, which increases with temperature.

The formation rates of H_2O and H_2O_2, which are reflected by the initial slopes of the curves, is also altered by the presence of CO in the ice. In the O_2-rich ice (1:4) the H_2O_2 column density shows the same behavior as seen in pure O_2 ices: a constant formation rate is followed by a sharp transition toward saturation (Chapter 4). For high concentration of CO in the ice, the H_2O_2 column density increases with a much lower rate and does not

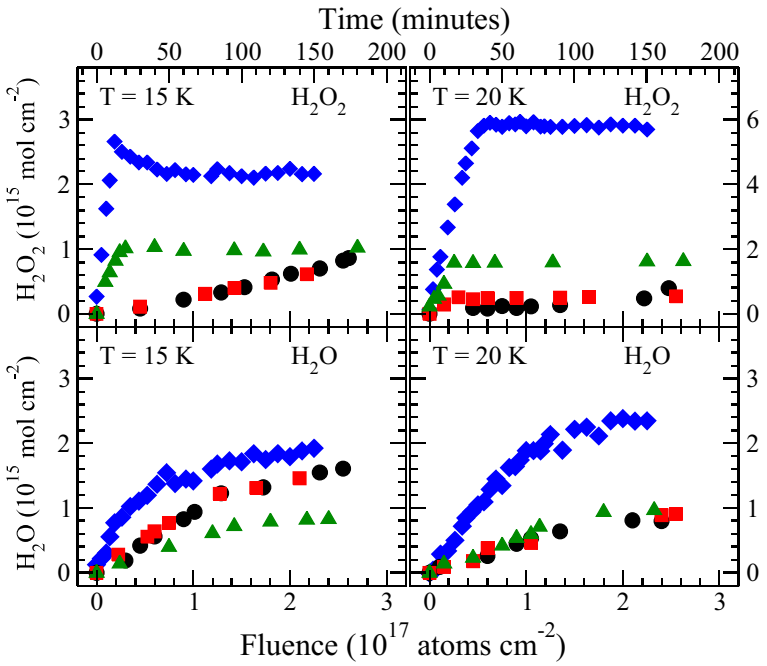

Figure 7.3 H_2O_2 (*top panels*) and H_2O (*bottom panels*) column densities as a function of the H-atom fluence and time of H-atom exposure at 15 K (*left panels*) and 20 K (*right panels*) for the three mixtures studied: CO:O_2 = 4:1 (*circle*), 1:1 (*square*), and 1:4 (*triangle*). For comparison, results from the hydrogenation of pure O_2 ice are plotted (*diamond*). Note different vertical scale for upper right panel.

appear to reach a steady state, even at the highest fluence. The H_2O_2 final yield increases with temperature, like for hydrogenation experiments of pure O_2 ice. The amount of H_2O_2 formed in the ice is inversely proportional to the amount of CO in the mixture, as expected.

In the case of CO-rich ice (4:1), a more efficient conversion of H_2O_2 ice into H_2O ice can explain the high H_2O final yield with respect to the O_2-rich ice experiment. In chapter 4 we showed that H_2O_2 is more effectively formed in the bulk of the ice (Chapter 4). However, the presence of CO in the ice limits the hydrogenation reactions to the surface of the ice. This means that a larger percentage of H_2O_2 formed at the surface of the ice is easily converted into H_2O. This may also explain the lower effective synthesis of H_2O_2 with the increase of the number of CO molecules in the ice. In addition, H_2O can be formed from OH radicals (see Fig. 7.1 and Chapter 5), which can also react to form CO_2 in our ices. The H_2O column density is constant through almost all our experiments. This is also the case for CO_2 as we will show in § 7.4.4 and indicative for a correlation between the formation channels of these two species.

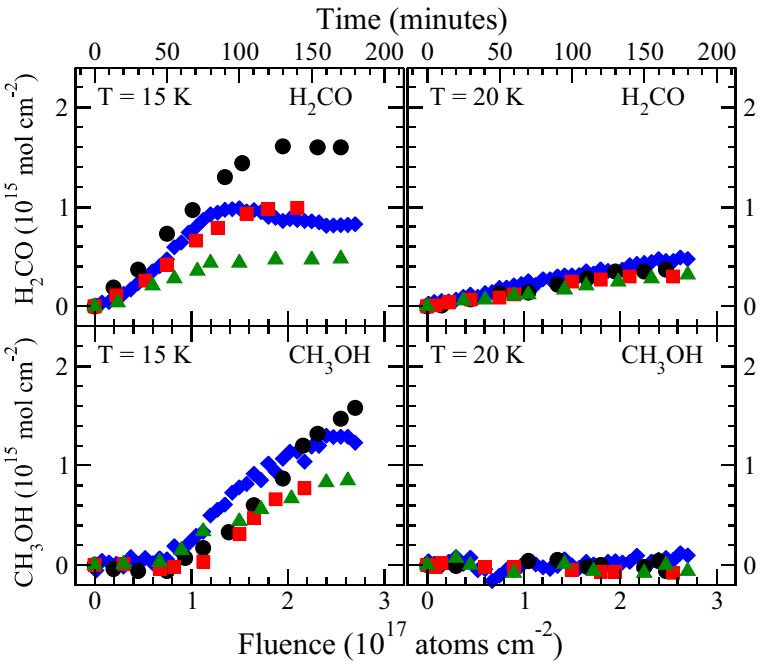

Figure 7.4 H_2CO (*top panels*) and CH_3OH (*bottom panels*) column densities as a function of the H-atom fluence and time of H-atom exposure at 15 K (*left panels*) and 20 K (*right panels*) for the three mixtures studied: $CO:O_2$ = 4:1 (*circle*), 1:1 (*square*), and 1:4 (*triangle*). For comparison, results from the hydrogenation of pure CO ice are plotted (*diamond*).

7.4.2 Hydrogenation of CO molecules

Figure 7.4 shows the H_2CO (*top panels*) and CH_3OH (*bottom panels*) column densities as a function of the H-atom fluence for the three different mixing ratios ($CO:O_2$ = 4:1 *circles*, 1:1 *squares* and 1:4 *triangles*) and two temperatures investigated (15 K left panels and 20 K right panels). For comparison, results from the hydrogenation of pure CO ice (Chapter 2) are also plotted (*diamonds*). For the hydrogenation of pure CO ice, the H-atom fluence is corrected according to recent H-atom flux measurements (Chapter 4), which improve the original H-atom flux estimation derived in Chapter 2. The hydrogenation of CO molecules in our mixtures shows the same behavior seen for pure CO ice in terms of temperature dependence (Chapter 2). An optimum in the final yield for H_2CO and CH_3OH is found at 15 K, while at 20 K no CH_3OH is formed and H_2CO has a low formation rate. The H_2CO and CH_3OH formation rates are hardly affected by the presence of O_2 in the ice (within the experimental uncertainties). The higher final yield for H_2CO and CH_3OH in the $CO:O_2$ = 4:1 experiment at 15 K compared to the pure CO ice

cannot be explained by only a difference in the effective H-atom flux. In this case, the presence of O_2 in the ice, as a minor component, increases the penetration depth of H atoms in the ice compared to pure CO and, therefore, the probability that the H atoms get trapped and react in the ice. However, if the O_2 concentration is increased in the 15 K ice, the final yield decreases for both H_2CO and CH_3OH molecules. Clearly, the formation of H_2CO is more sensitive to the O_2 concentration in the ice than CH_3OH. As we saw for the hydrogenation of O_2 ice, the intermediate products (H_2O_2 and H_2CO respectively) are more efficiently converted in the final products (H_2O and CH_3OH, respectively), when the ices are mixed.

7.4.3 Competition between the CO and O_2 channel

The results presented in the former sections reflect the competition between the two channels CO vs. O_2, as shown in the left and right part of Fig. 7.1. It is clear from the experimental results that the presence of one component in the ice influences the reactivity of the other component. The formation rate of the CO hydrogenation reaction products is less affected by the presence of O_2 than the O_2 hydrogenation reaction products are affected by the presence of CO. This can be explained by the lower penetration depth of H atoms in CO ice and by the formation of CO_2 as an additional product, since OH radicals, formed through the O_2 channel, are used to yield CO_2 instead of H_2O and H_2O_2.

In a CO-rich environment at 15 K, the presence of O_2 molecules enhances the production of H_2CO and CH_3OH, since H atoms can penetrate deeper in the ice than in the pure CO ice experiment. However, the formation rate of the final products seems not to be affected by the presence of the O_2 molecules in the ice. Moreover, in a CO-rich ice the formation of H_2O_2 is limited by the small amount of O_2 molecules in the ice, by the amount of OH radicals used to form CO_2 and by the lower penetration depth of H atoms in the ice, caused by the presence of CO molecules. H_2O_2 ice is also more efficiently converted to H_2O on the surface of the ice. This explains the high final yield for H_2O in a CO-rich environment at 15 K.

In a O_2-rich environment at 15 K, the formation of H_2CO and CH_3OH is limited by the small amount of CO molecules, which limits the formation of H_2O_2 and H_2O, since the penetration depth of H-atoms is lower than in the pure O_2 ice experiment.

At 20 K, the CO channel is not efficient, although the H atoms penetrate deep in the ice; at this temperature H atoms prefer to react with O_2 molecules. Also in this case the final yields for H_2O_2 and H_2O are lower than those in the pure O_2 ice experiment.

7.4.4 Formation of solid CO_2

Figure 7.5 shows the CO_2 column density as a function of the H-atom fluence, confirming the CO_2 formation for the three different mixing ratios and two temperatures investigated. Neither the CO_2 formation rate nor its final yield depend significantly on either temperature or mixing ratio for the values studied here. Such a behavior is unexpected, since the

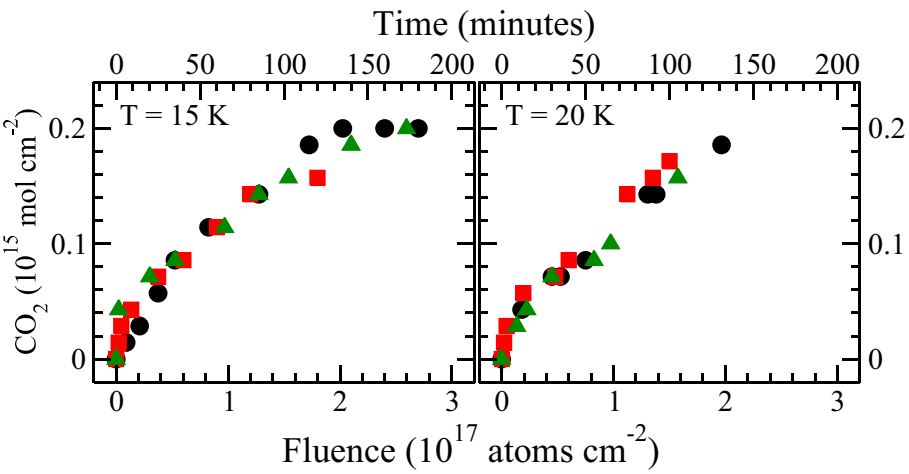

Figure 7.5 CO_2 column density as a function of the H-atom fluence and time of H-atom exposure at 15 K (*left*) and 20 K (*right*) for the three mixtures studied: CO:O_2 = 4:1 (*circle*), 1:1 (*square*), and 1:4 (*triangle*).

separate reaction routes CO + H and O_2 + H clearly depend on temperature, as shown in Chapters 2 and 4. The limiting factor for the CO_2 synthesis in our experiments is, therefore, the amount of ice that can be penetrated by H atoms, which is only a few monolayers. This is caused by the presence of CO molecules affecting the penetration depth of the H atoms in the ice (Chapter 2). Thus, the amount of CO_2 formed in all our experiments is always less than a monolayer. CO_2 subsequently does not contribute to further molecular synthesis in the ice upon ongoing hydrogenation. Bisschop et al. (2007b) showed experimentally that CO_2 does not react with H atoms and is a stable molecule under interstellar ice analogue conditions.

Figure 7.1 summarizes schematically the reaction network which leads to the formation of solid CO_2 starting from the combination of the CO + H and O_2 + H channels. Analyzing the species present in our ice after H-atom addition we can identify which reaction channel is most likely responsible for the formation of solid CO_2 ice. The hydrogenation of the HO-CO intermediate (*black arrow* in the center of Fig. 7.1) should not occur in our experiments, since HCOOH is not detected in the infrared spectra. Density functional calculations (Goumans et al. 2008), confirmed by our previous experimental results (Chapter 8), suggest that the final products from the hydrogenation of the HO-CO complex have a purely statistical branching ratio. Therefore, HCOOH should be detected in the ice as well if CO_2 would be produced through this route, and this is not the case.

The oxidation of solid CO (*dashed arrow*) is also not likely to be the main formation reaction channel, since O_3, which would indirectly prove the presence of abundant O atoms in the ice, is not observed. O_3 ice has been detected in pure O_2 hydrogenation experiments only for temperatures higher than 25 K, when the penetration depth of the H

atoms is higher than a few monolayers and the O_2 molecules are most likely more mobile (Chapter 4). The hydrogenation of O_3 ice (Chapter 6) is therefore not considered here. Furthermore, Roser et al. (2001) tentatively observed CO_2 formation through this channel only during the warm up of the ice and when CO molecules and O atoms were covered by a thick layer of H_2O ice, which allows the reactants to remain trapped in the ice for $T > 100$ K. The CO + O reaction contributes at best at high temperatures. Reaction HCO + O (*dotted arrow*) should also be ruled out, since HCO radicals prefer to react in a barrierless manner with H atoms forming H_2CO rather than with O atoms, as shown in Chapter 2 and 8. Furthermore, O atoms are not abundant in our ices.

At low temperatures CO_2 is therefore formed through the direct dissociation of the HO-CO complex in the ice (*black arrow*). The HO-CO complex is efficiently dissociated and, therefore, is not detected in our infrared spectra as a stable species. In chapter 4 we observed this complex only in a water-rich environment. H-bonding should, indeed, improve coupling and heat dissipation through the ice, which stabilizes the HO-CO complex more easily in a polar environment than in an apolar one. Our ice is mainly composed of CO and O_2, with a polar component on the surface of the ice. The amount of the HO-CO intermediate stabilized in the polar ice is also under the detection limit. Therefore, in a water-poor ice the competition between dissociation and further hydrogenation of the HO-CO complex is in favor of the dissociation. H_2O is also formed through hydrogenation of the OH radicals. Hence, the formation of CO_2 is linked to the formation of H_2O in the ice. This is consistent with the presence of CO_2 in polar interstellar ice mantles.

7.5 Astrophysical implications

Recently, results from *Spitzer Space Telescope* observations (Whittet et al. 2007, Pontoppidan 2006, Pontoppidan et al. 2008) have shown that the formation of CO_2 in dark quiescent clouds occurs in two distinct phases. In the early stages, CO_2 forms together with H_2O on the surface of the interstellar dust grains, creating a polar ice mantle. A second phase in the CO_2 formation occurs during the heavy freeze-out of CO. During this second phase, a H_2O-poor ice is formed.

Our experimental results indeed make it likely that CO_2 and H_2O are formed together in the early stages of the clouds through surface reactions assuming that both CO and OH are present in sufficiently high abundances. H_2O ice forms from continued hydrogenation of OH radicals formed on the surface of the dust grains. Alternatively, OH radicals can react with nearby CO molecules, which are present in small amounts in the ice before the strong CO freeze-out phase, forming CO_2 ice through the direct dissociation of the HO-CO intermediate. CO_2 can be also formed at low temperatures through the hydrogenation of the HO-CO complex, which can lead to the formation of HCOOH and H_2O + CO as well as CO_2 + H_2. The concentration of CO in the ice with respect to H atoms determines the probability of OH to react with a CO molecule or with another H atom.

In the second stage, during the heavy CO freeze-out, the gas density is $>10^5$ cm^{-3} and the CO accretion rate could be as high as, or even higher than, the H-atom accretion rate, which makes CO more abundant on the surface than H atoms. OH radicals will

therefore more likely react with a nearby CO molecule than with H atoms. CO_2 can thus be efficiently formed through the dissociation or further hydrogenation of the HO-CO complex, while just little H_2O ice formed.

Energetic processing (UV irradiation and cosmic ray-induced photons) of polar and apolar ices is also an efficient mechanism for CO_2 formation for specific environments (Hagen et al. 1979, Mennella et al. 2004, Mennella et al. 2006, Loeffler et al. 2005, Ioppolo et al. 2009). All these channels could contribute to the total CO_2 column density component observed in quiescent clouds.

The experiments presented here are designed to test a possible CO_2 formation route (thermal CO + OH) under interstellar ice analogue conditions rather than simulate a complete realistic interstellar ice evolution. Although our experiments do not exclude other possible CO_2 formation mechanisms, they show that the dissociation of the HO-CO complex is efficient and can contribute to explain the presence of CO_2 in polar and apolar interstellar ices at low temperatures in absence of UV irradiation.

7.6 Conclusions

The present laboratory study shows that the CO and O_2 channels influence each others final product yields, when CO and O_2 molecules are mixed and hydrogenated at low temperature (15 and 20 K). The formation rate for all the final products is found to be less sensitive on the mixture composition than the final yield. The penetration depth of the incoming H atoms is the main limiting factor. It depends on the composition of the ice and decreases when the amount of CO in the ice increases. Our results show that the formation rates found for H_2CO, CH_3OH, H_2O_2 and H_2O are similar within the experimental uncertainties to those found studying the isolated CO and O_2 hydrogenation channels corrected for the reduced effective H-atom fluxes. Therefore, the formation rates found in the isolated studies of the CO + H and O_2 + H channels are still valid for use in astrochemical models.

The formation of CO_2 from the reaction CO + OH is found here. CO_2 is efficiently formed under our laboratory conditions and no dependence on temperature or ice composition is found. The formation of CO_2 is linked to the formation of H_2O and, therefore, competes with the O_2 hydrogenation channel in our experiments. The competition of these two channels, together with the composition of the ice and the penetration depth of H atoms into the ice, explains the differences in the H_2O_2 and H_2O formation rate between our results and the hydrogenation of pure O_2 ice.

Figure 7.1 shows how the H_2O formation through the $O/O_2/O_3$ + H channels is linked to the CO_2 formation. Here we investigated only the O_2 + H channel, even though OH radicals can be efficiently formed on dust grains through all H_2O formation channels as well as through the photodissociation of H_2O and CH_3OH ice. Thus, our experimental result on the efficiency of the CO + OH channel at low temperature has important astrophysical implications on the formation of solid CO_2 in cold dense molecular clouds shielded from strong UV fields and are consistent with the observation of solid CO_2 in H_2O-rich environments.